

HOSTED BY



Contents lists available at ScienceDirect

Journal of King Saud University – Science

journal homepage: www.sciencedirect.com

Original article

A cytological efficiency evaluation study of rare earth and carbon based material against breast cancer cells



Rizwan Wahab*, Maqsood A.Siddiqui, Javed Ahmad, Quaiser Saquib, Abdulaziz A. Al-Khedhairi

Chair for DNA Research, Zoology Department, College of Science, King Saud University, Riyadh 11451, Saudi Arabia

ARTICLE INFO

Article history:

Received 28 May 2023

Revised 21 June 2023

Accepted 26 August 2023

Available online 29 August 2023

Keywords:

Functional CNTs
Neodymium oxide
MCF-7 cells
ROS
RT-PCR

ABSTRACT

Cancer is a denying disease and among a number of cancers types, breast cancer is usual in females, and affect the worldwide. For these reason, the work presented here to show the cytological and apoptotic evaluation of breast (MCF-7) cancer cells with functional carbon nanotubes (FCNTs) and rare earth material (REE) neodymium oxide. At initial, the CNTs were functionalized with acid treatment method, whereas neodymium oxide nanorods (Nd₂O₃NRs) were synthesized and characterized. The Fourier transform infrared (FTIR) was used to check the functional characteristics of CNTs, whereas crystalline property, particle size and phase of Nd₂O₃NRs were confirmed via X-ray diffraction pattern (XRD) respectively. The morphologies of nanostructures were observed via scanning electron microscopy (SEM) and transmission electron microscopy (TEM) correspondingly. The cytological efficiencies of cancer cells were evaluated with FCNTs and Nd₂O₃NRs at varied concentrations (1, 2, 5, 10, 25, 50 and 100 µg/mL) verified via MTT and NRU assays. The ROS was enhanced in Nd₂O₃NRs as compared to CNTs with control. The gene expression study were also conducted and it unveils that the level of mRNA with Nd₂O₃NRs were upregulated and it depicts the apoptosis in cells. The study designates that the Nd₂O₃NRs are more efficient as compared to the functional CNTs with MCF-7 cancer cell.

© 2023 The Author(s). Published by Elsevier B.V. on behalf of King Saud University. This is an open access article under the CC BY-NC-ND license (<http://creativecommons.org/licenses/by-nc-nd/4.0/>).

1. Introduction

Among various types of cancers, the breast cancer is very common and deadliest after the lung cancer especially in female candidate. This shattering disease is increasing rapidly and affected world widely (Alshareeda et al., 2023). As according to the report by World health organization (WHO), ~2.3 million women diagnosed with breast cancer and 685,000 deaths globally and grasp more and more (WHO fact-sheet detail for breast cancer 2021). A number of cases increase very rapidly such as ~421,000 cases were diagnosed for cancers in 2008, ~49,500 cases were found in 2009–2010 only in Europe (Ferlay et al., 2008). An estimated data shows that ~42,170 women in U.S. to die in 2020 (Breast Cancer Facts & Figures (2019)–2020) and affected word widely. As per the WHO, in

Saudi Arabia, 3629 new cases of breast cancer for all ages were reported in 2018 (Alshareeda et al., 2023; Alghamdi et al., 2021). A number of therapies and surgical options were opted to control this devastating disease such as radio, Chemo, proton beam, hormone, drug and immune therapy etc. Including to these, the surgical options were also opted to remove the cancer cells from the particular organ of the body (Wahab et al., 2022).

Numerous options are available to remove the cancer cells from the body but all these options are costly and not easy to opt for low income or deprived families (Wahab et al., 2021). The nano technology is the best alternative to treat such disease at a very low cost, effective against cancer cells not to affect the other organs in the body (Al-Khedhairi and Wahab, 2022). In this continuation, a REE, which is generally known as toxic material in nature and can be directly or indirectly affect to human beings (Brouziotis et al., 2022). Among a range of REEs, neodymium is one of the material, which exhibit magnetic properties and thats why largely applied in different sectors such as audio, phones, magnets, speakers, hard drives in computers, catalysts etc (München et al., 2017, Tang et al., 2020 and Ramos et al., 2016). Due to the larger utility and demand in different sectors, the neodymium production is enhances very fast with its annual turnover is 7,300 tons and accounts in production as a fourth largest REEs in the world

* Corresponding author at: College of Science, Zoology Department, P.O. Box 2455, King Saud University, Riyadh 11451, Saudi Arabia.

E-mail address: rwahab@ksu.edu.sa (R. Wahab).

Peer review under responsibility of King Saud University.



Production and hosting by Elsevier

(Majhi and Yadav, 2022). A number of chemical toxicities studied were conducted and documented in detail (Bergsten-Torralba et al., 2022; Kurvet et al., 2017) but very few research is available that show the effect of toxicities studies on human beings.

Including the oxide based material, the carbon nanotubes, which are classified as multiwalled (diameter 10–15 nm, length 2–4 μm) and single walled (diameter $\sim 0.2\text{--}0.3$ nm and length extends up to 1–2 μm) structure, exhibit unique structural and chemical properties, high aspect ratios, large surface areas, enough surface and chemical functionalities etc (Wahab et al., 2009). The CNTs exhibit multi-purpose, vast applications and are largely applied in various directions such as chemical, biological, sensors and energy storage etc. (Venkataraman et al., 2019). Ample studies are documented related to the applications CNTs in electronics but a few studies are available to use CNTs as a biological or biomedical purposes with cytotoxicity studies against cancer cells (Prajapati et al., 2022). The literature available in this directions for instance CNTs were utilized for cytological study against human lung epithelial cells (A549), murine macrophages (J774), mesenchymal stem cells (MSCs) (Kumarathasan et al., 2015; Czarnecka et al., 2020). MWCNTs were employed for to examine the cytotoxicity against rat alveolar macrophages (NR8383) cells with inhalation toxicity (Fujita et al., 2020).

The purpose of the current study is to compare the cytotoxicity studies with FCNTs and $\text{Nd}_2\text{O}_3\text{NRs}$ against MCF-7 cells with varied concentrations of the material. The $\text{Nd}_2\text{O}_3\text{NRs}$ were formed with solution method and characterized. The morphology of cultured and treated cells were retrieved via microscopy. The cytotoxicity's of $\text{Nd}_2\text{O}_3\text{NRs}$ and functional CNTs were tested via 3-[4,5-dimethylthiazol-2-yl]-2,5 diphenyl tetrazolium bromide (MTT) and Neutral Red Uptake (NRU) assays. The reactive oxygen species (ROS) and real-time reverse transcription–polymerase chain reaction (RT-PCR) study were also performed to show the role of $\text{Nd}_2\text{O}_3\text{NRs}$ and carbon based materials on cancer cells.

2. Experimental

2.1. Material and methods

2.1.1. Functionalization of CNTs

The raw CNTs were purchased from Sigma Aldrich chemical corporation, U.S.A, cleansed and functionalized with concentrated acid reflux method (HNO_3 and H_2SO_4) as described earlier (Wahab et al., 2009). The product was transferred in a centrifuge tubes (~ 50 mL capacity) and centrifuge (Eppendorf, 5430R, Centrifuge, Germany) at 3000 rpm for 3 min and dried at room temperature. The functional CNTs were analyzed in terms of their morphological and chemical characteristics.

2.1.2. Synthesis of neodymium oxide/REEs

The REE/neodymium oxide nanostructures were formed with the use of neodymium nitrate ($\text{Nd}(\text{NO}_3)_3 \cdot 6\text{H}_2\text{O}$) and sodium hydroxide (NaOH) (Sigma Aldrich Chem Co. U.S.A) as described earlier with minor alteration (Ahmad et al., 2022). At initial, neodymium nitrate ($\text{Nd}(\text{NO}_3)_3 \cdot 6\text{H}_2\text{O}$, ~ 0.3 M) was dissolved in double distilled water in a 100 mL capacity beaker. When the $\text{Nd}(\text{NO}_3)_3 \cdot 6\text{H}_2\text{O}$ was completely dissolved, NaOH (0.3 M in 100 mL) was added and assorted softly. The pH of this solution was checked and it touch to 12.8. The aqueous solution of $\text{Nd}(\text{NO}_3)_3 \cdot 6\text{H}_2\text{O}$ and NaOH was moved for heating in glass pot and heated at 80°C for 4 h. After the completion of the reaction, the aqueous powder product was centrifuged at 3000 rpm for 3 min (Eppendorf, 5430R, Centrifuge, Germany) to remove the impurities during the reaction process, afterward, it was transferred on to glass petri dishes and

dried at 60°C in an oven. The dried powder was kept for further analysis.

2.1.3. Characterizations

The formed powders crystallinity, phases of miller indices and size of crystallite were examined via XRD (PAN analytical XPert Pro, U.S.A.) with $\text{Cu}_{K\alpha}$ source ($\lambda = 1.54178 \text{ \AA}$) from 20 to 80° with 6° angle rotation/min speed. The general structural detail of the prepared product were analyzed via SEM (JSM-6380 LA, Japan) and TEM (JEOL JEM JSM 2010, Japan at 200 kV current) as described earlier (Wahab et al., 2022). The functional assessment of the prepared products were analyzed via FTIR (Perkin Elmer FTIR Spectrum-100, U.S.A.) spectroscopy from 400 to 4000 cm^{-1} .

2.2. Cell culture

The culture of breast cancer cells (MCF-7) was conducted with using a medium (DM EM/MEM) including 12% fetal bovine serum (FBS), 0.2% sodium bicarbonate, and antibiotic–antimycotic solution (100 X, 1 mL/100 mL) with humid environment ($5\% \text{ CO}_2$ & $95\% \text{ O}_2$) at 37°C . As reported (Siddiqui et al., 2008), the viability of cells were estimated by trypan blue dye and it express that more

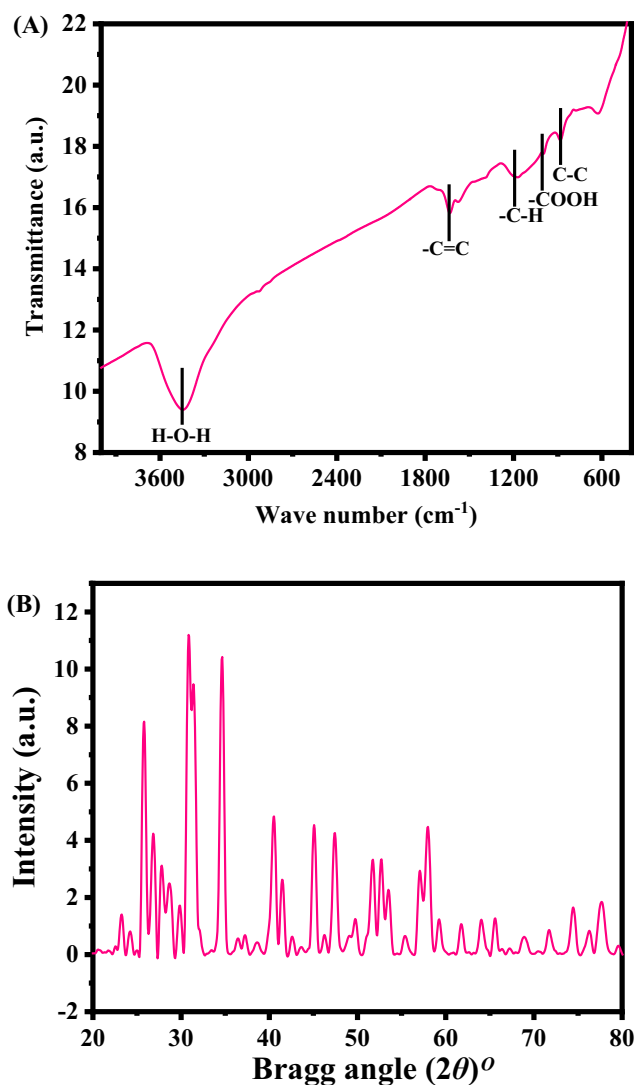


Fig. 1. (A) FTIR spectroscopy of Functional CNTs (FCNTs), (B) XRD spectra of neodymium oxide (Nd_2O_3).

than 95% achieved viability of the cells and utilized. The cells were used between 10 and 12 passages to treat cells with FCNTs and Nd₂O₃NRs. Initially, the stock solution (10 mg/ml) of FCNTs and Nd₂O₃NRs was prepared at high concentration and further diluted at desired varied concentrations for the exposure of cells. The cells were plated in 96-wells as per the experimental requirement.

2.3. Reagents and consumables for biological study

The MTT assay was procured from Sigma Chem.Co.USA and castoff without any further modification except dilution. Dulbecco's Modified Eagle Medium (DMEM) and MEM culture medium, antibiotics-antimycotic and FBS were bought from Invitrogen, USA. The plastic wares and other consumables products for cells culture were used from Nunc, Denmark.

2.4. MTT assay

The breast cancer cells viabilities with and without use of FCNTs and Nd₂O₃NRs were measured with MTT assays (Siddiqui et al., 2008, Mosmann, 1983). For this, at initial the cells were sowed in 96 well plates (rate of 1×10^4 /well) with permissible to follow for 24 h at 37 °C with humid environment. Here, the cells were completely exposed with FCNTs and Nd₂O₃NRs 1–100 µg/mL for 24 h, mixed the MTT (5 mg/mL in PBS) with rate of 10 µL/well in 100 µL of cell suspension and cells were further incubated for 4 h. As the incubation was reached to their completion, the well plate's solution was with draw from the pipette and in these wells ~200 µL of DMSO was mixed for to aspirate the formazan product.

Solutions optical characteristic was checked at 550 nm with micro-plate reader (Multiskan Ex, Thermo Scientific, Finland). With treated samples, the control cells were also measured as a reference and to run with same conditions. The maximum absorbance depends upon used solvent in sample solution and the level of viability of cells % was calculated as per the equations mentioned below:

$$\% \text{ viability} = [(\text{total cells} - \text{viable cells}) / \text{total cells}] \times 100$$

2.5. NRU assay

Including the MTT assay, the treated and untreated cells cytotoxic optical characteristic were also confirmed via neutral red uptake (NRU) assay (Borenfreund and Puerner, 1985; Siddiqui et al., 2010). The MCF-7 cells (1×10^4 /well) were sowed in a specified 96 well plates. Once the cells were completely grown, exposed with both samples at desired conc (1–100 µg/mL) and to kept for 24 h in an incubator. After the exposure was finished, the cells were again incubated in NR medium (50 µg/mL) for 3 h. Then cells were completely washed and dye were extracted from both samples in 1% acetic acid and 50% ethanol solution. The develop color was checked at 540 nm.

2.6. Reactive oxygen species (ROS)

The ROS generation were measured with the use of 2,7-dichloro dihydrofluoresce in diacetate (DCFH-DA) dye; procured from Sigma Aldrich, USA) dye as a fluorescence agent as described

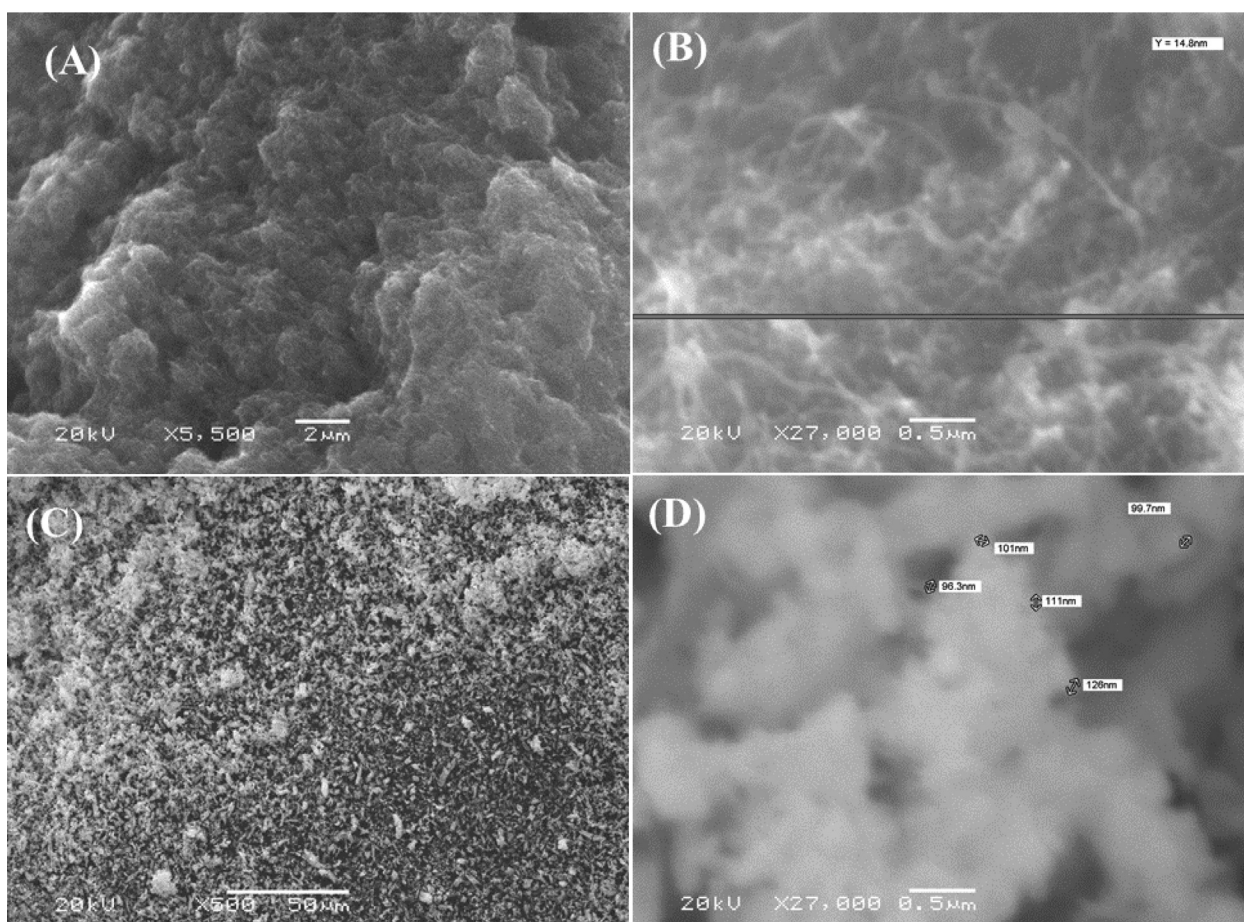


Fig. 2. SEM images of Functional CNTs (FCNTs) (low (A) and high (B) magnified) and Nd₂O₃NRs (size ~90–120 nm) (low (C) and high (D) magnified scale images respectively). The images depicts the FCNTs average size of each nanotube diameter is ~10–15 nm, whereas length is about 2–3 µm.

method previously (Siddiqui et al., 2013). The cells were exposed with both nanostructures for 24 h and thereafter, cells were rinsed well with PBS and further nurtured for 30 min in DCFH-DA (20 μM) in dark place at 37 $^{\circ}\text{C}$. The reaction of DCFH-DA dye with cells as control and treated (FCNTs and $\text{Nd}_2\text{O}_3\text{NRs}$) cells were completed, and examined with using fluorescence microscope.

2.7. mRNA expressions with cancer cells (MCF-7)

The extraction of RNA was accomplished with cultured cells of MCF-7 cells in a 6-well plates control and treated samples at concentration of 50 $\mu\text{g}/\text{mL}$ for 24 h. For this process, the RNeasy mini Kit (Qiagen) was used to mined the RNA as per protocol instructed from manufacturer's. The cDNA was synthesized from the treated and untreated cells taking 1 μg of RNA by Reverse Transcriptase kit using MLV reverse transcriptase (GE Health Care, UK) as described protocol. The RT-PCR was completed on Roche[®] Light Cycler[®]480 (96-well block) (USA) followed with cycling program as recommended (Humes et al., 2017).

3. Result and discussion

3.1. FTIR spectroscopy

The functional characteristics of the black powder was analyzed via FTIR spectroscopy and the obtained data illustrated as Fig. 1(a). A number of bands were observed at different positions, the acid treated or functional CNTs signals shows at 3442 cm^{-1} , depicts the H–O–H stretching vibration mode whereas signal at 1630 cm^{-1} denotes the C = C group of CNTs. The other band assigned at 1201 cm^{-1} , which assign to C–H stretching band

(Fig. 1(a)). Including to these the carboxylic (COOH-) group was observed at 1014 cm^{-1} , whereas C–C band signifies at 885 cm^{-1} (Wahab et al., 2009) (Fig. 1(a)). The observed bands and their assigned peak positions signifies that the CNTs are functional with carboxylic (–COOH) group.

3.2. X-ray diffraction pattern (XRD)

Fig. 1(b) shows the XRD pattern of synthesized powder, which represent the indexed and allocated peaks are analogous to

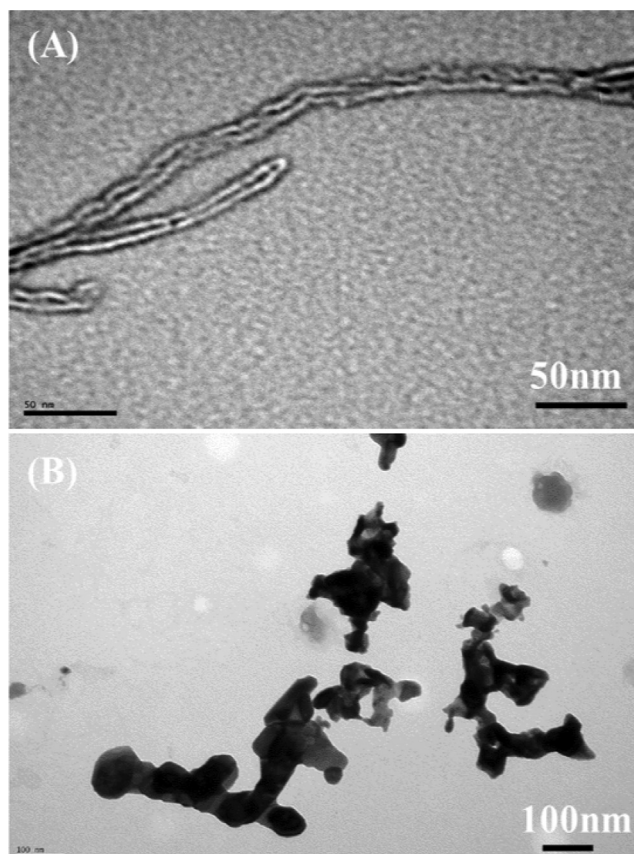


Fig. 3. TEM images displayed the FCNTs ($D \sim 10\text{--}15$ nm, $L \sim 2\text{--}3$ μm) (A) and $\text{Nd}_2\text{O}_3\text{NRs}$ (size $\sim 90\text{--}120$ nm) (B).

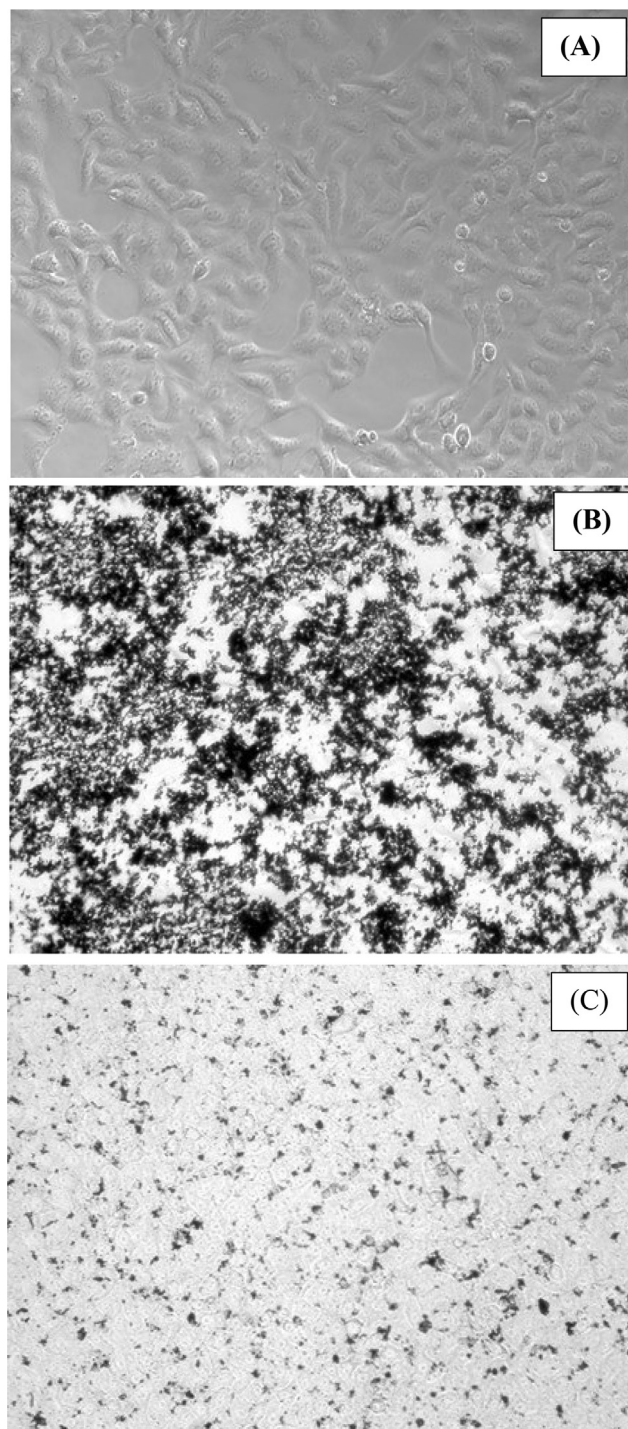


Fig. 4. Morphological change in MCF-7 cells (Control-A) with exposed to Functional CNTs (B) and $\text{Nd}_2\text{O}_3\text{NRs}$ (C) for 24 h. Images were captured with inverted microscope.

Nd₂O₃ and in accordance with hexagonal structure of Nd₂O₃ (JCPDS card no.41–1089). The average crystallite size was ~15 ± 1 nm calculated from scherrer equation and correspondents to the earlier literature (Ahmad et al 2022).

3.3. SEM results

The morphology of the processed powder was scanned with SEM and the recovered images are illustrated as Fig. 2. The images captured at low magnification scale (Fig. 2A) seems a number of particles were arranged and aggregated with each other.. Also to know the more clear detail, the data in term of image was captured at high magnification (Fig. 2B). A number of rope like structures are seen at the surface with diameter nearly from 10-15 nm and length goes to 2-3 μm. In Fig. 2C, Shows that a number of plates or rods shaped structures are appeared on the whole surfaces and the estimated average size of an individual rod diameter is ~90–120 nm whereas length goes up to 1–2 μm (Fig. 2D). The obtained SEM data is well consistent with the X-ray diffraction data (Fig. 1B).

3.4. TEM results

Further, the assessment for morphology, both powders were also analyzed with TEM and the obtained data is presented as Fig. 3. Fig. 3(A) shows the TEM image of FCNTs, which represents the diameter of each individual nanotube is ~10–15 nm and length reaches to 2–3 μm. Fig. 3(B) represent the TEM image of Nd₂O₃ NRs where a number of several particles are seen on the surface and its shows that size of an individual particle, seems to very similar to the SEM images (D=~90–120 nm, L=~1–2 μm) and are fully consistent with Fig. 2.

3.5. Morphology of MCF-7 cancer cells and their effect with nanostructures

The cells were cultured as described protocol in material and method and the morphological study was observed via microscopy at 24 h incubation periods with a selected concentration (50 and 100 μg/mL) ranges of FCNTs and Nd₂O₃NRs (Fig. 4). The captured

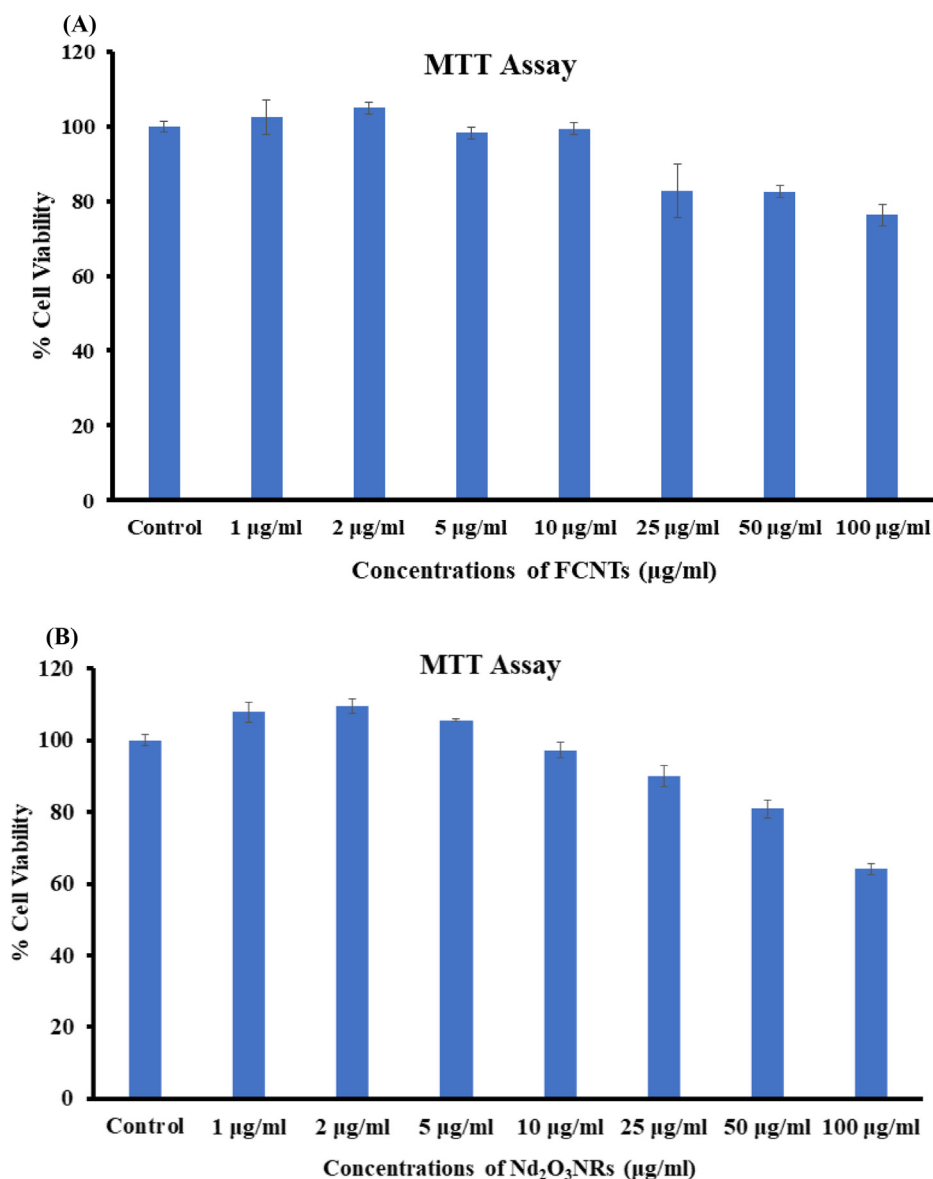


Fig. 5. The cytotoxicity via MTT assay in MCF-7 cells following the exposure with FCNTs (A) and Nd₂O₃NRs (B) for 24 h. The experiments were conducted in triplicate manner (Mean ± SD triplicate).

image of MCF-7 cancer cells were utilized as control (Fig. 4A) whereas others images were captured with treated samples at different concentrations of FCNTs (Fig. 4B) and Nd₂O₃NRs (Fig. 4C) respectively. From the images, it seems that the cells are nucleated and when the confluences reached to their optimum level (~70–80%) treated with FCNTs and Nd₂O₃NRs at 100 µg/mL and analyzed. The images reveals that there is no remarkable change was noticed at an initial range of concentration of 25 µg/mL (data not shown), but when the concentration of FCNTs and Nd₂O₃NRs upsurges to 50 to 100 µg/mL, the growth of cells were much influenced and it appears to be dose dependent (Fig. 4). The microscopic images authenticated that the cells were damaged with the incorporation of FCNTs and Nd₂O₃NRs correspondingly (Vantangoli et al., 2015).

3.6. The cytotoxicity via MTT assay

As described in the material and method section, the untreated (control) breast cancer cells (MCF-7) and treated cells (MCF-7 cells with FCNTs and Nd₂O₃NRs samples were exposed in a range of dif-

ferent conc from 1 to 100 µg/ml for 24 h incubation. The cytotoxicity's were examined via MTT assay. The optical densities data shows the viabilities of cancer cells were diminished with the incorporation of nano structures. In case of FCNTs, the MCF-7 cells viability reduced in MTT assay observation at 24 h 101%, 102%, 102%, 103%, 89%, 79% and 63% (Fig. 5A) for the conc 1, 2, 5, 10, 25, 50 and 100 µg/mL correspondingly (p < 0.05 for each). In case of Nd₂O₃NRs, the MCF-7 cells viability, MTT assay was declines at 24 h 101%, 101%, 98%, 94%, 62%, 54% and 49% (Fig. 5B) for the conc of 1, 2, 5, 10, 25, 50 and 100 µg/mL correspondingly (p < 0.05 for each). The data's shows that the cells viabilities were not much affected with FCNTs at initial conc., whereas once the doses were increased, the Nd₂O₃NRs exceeded to their optimum level, the cytotoxicity's were much influenced as compared to FCNTs.

3.7. The cytotoxicity via NRU assay

Apart from the MTT assay, the cytotoxic measurements were also verified treated (MCF-7 cells with FCNTs and Nd₂O₃NRs) and

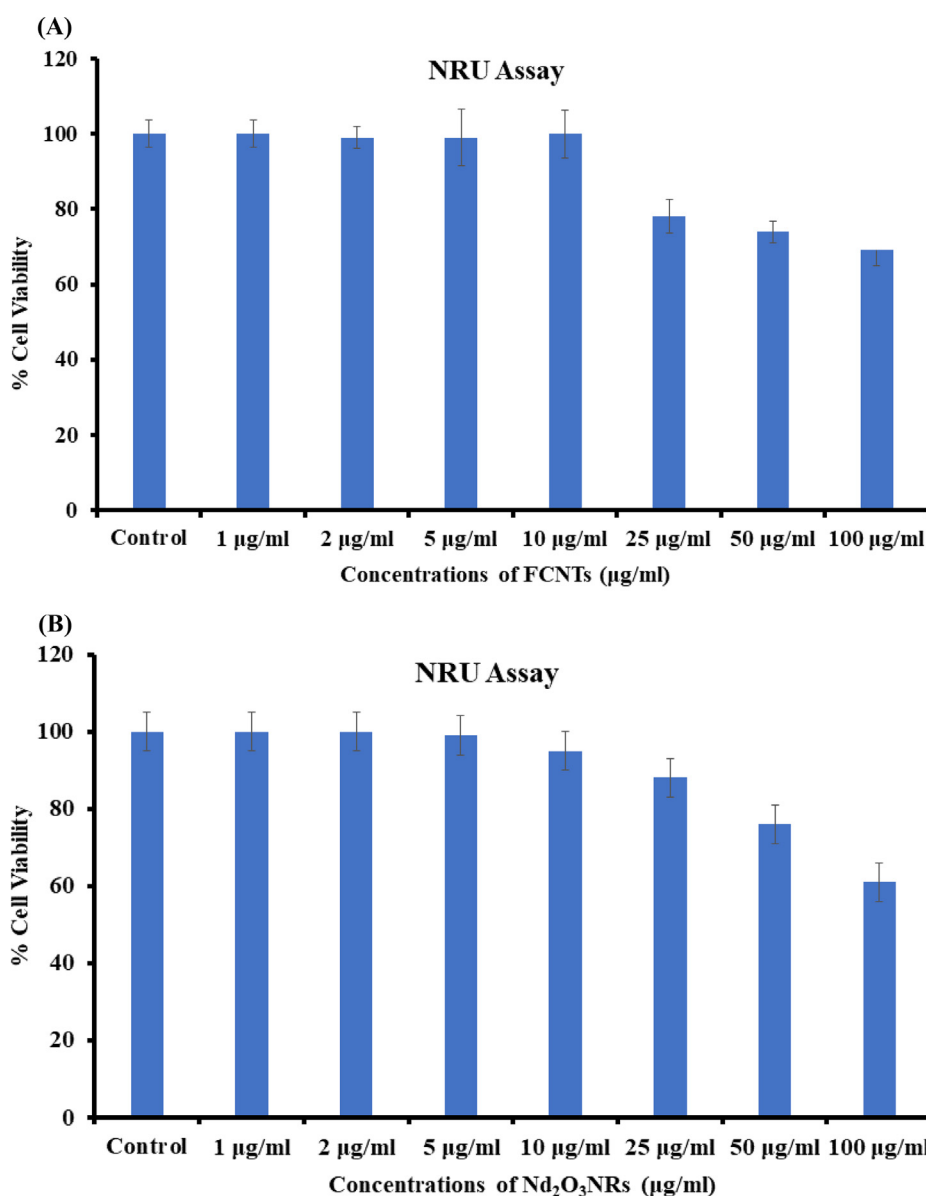


Fig. 6. The cytotoxicity via NRU assay in MCF-7 cells following the exposure of FCNTs (A) and Nd₂O₃NRs (B) for 24 h. The experiments were conducted in triplicate manner (Mean ± SD triplicate).

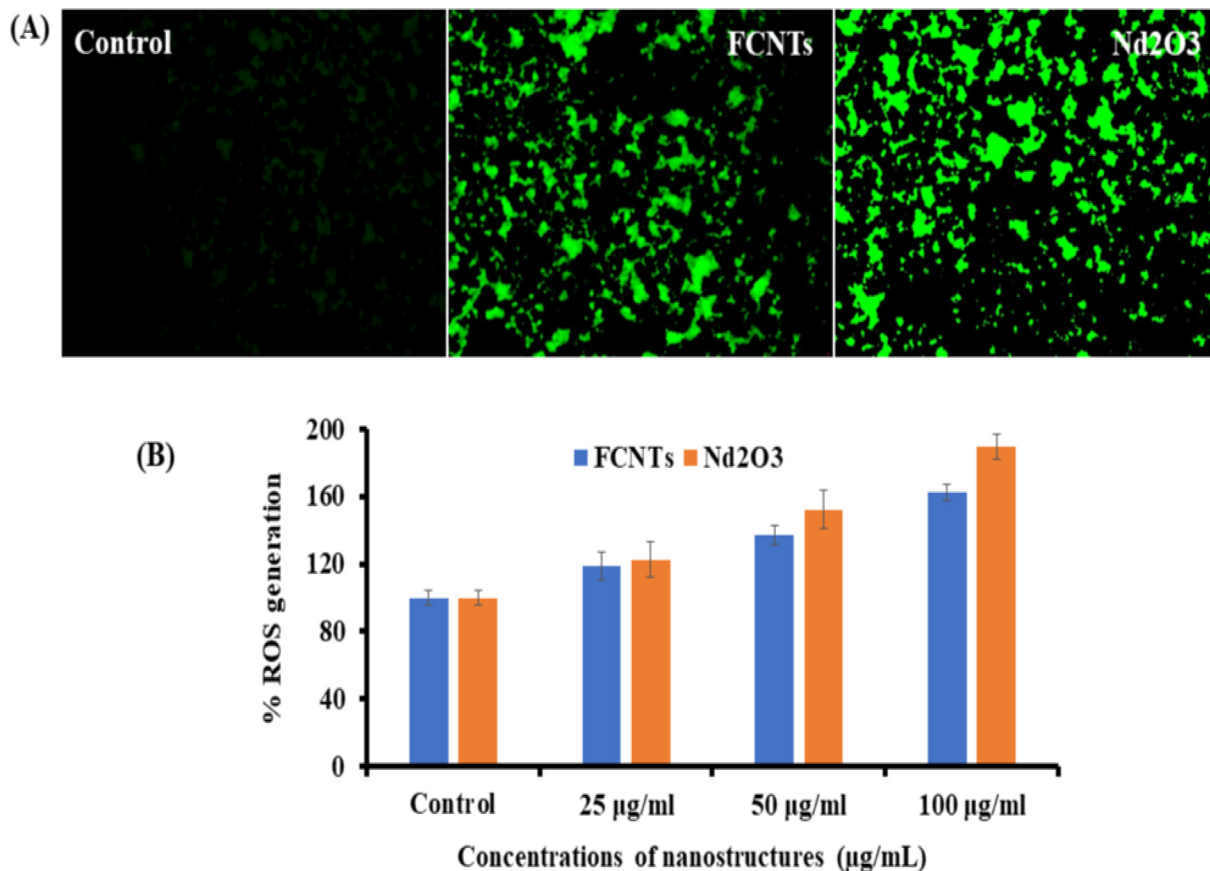


Fig. 7. (A) Representative images of FCNTs and Nd₂O₃NRs induced ROS in MCF-7 cells exposed for 24 h. (B) % change in ROS generation with MCF-7 at varied concentrations of FCNTs and Nd₂O₃NRs for 24 h.

untreated (Control) sample via NRU assays. A similar observation were also found in NRU assays. As described in the MTT section, the NRU data also in consistent and shows that that the viabilities of cancer cells at initial doses of FCNTs and Nd₂O₃NRs were not much affected, as the doses increases, the cancer cells growth were retarded. In case of FCNTs, for the MCF-7 cells, NRU assay was falls

at 24 h 102%, 101%, 104%, 100%, 91%, 84% and 60% (Fig. 6A) for the concentrations of 1, 2, 5, 10, 25, 50 and 100 µg/mL correspondingly (p < 0.05 for each). In case of Nd₂O₃NRs, for the MCF-7 cells, NRU assay was diminutions at 24 h 98%, 97%, 93%, 90%, 69%, 64% and 51% (Fig. 6B) for the concentrations of 1, 2, 5, 10, 25, 50 and 100 µg/mL correspondingly (p < 0.05 for each).

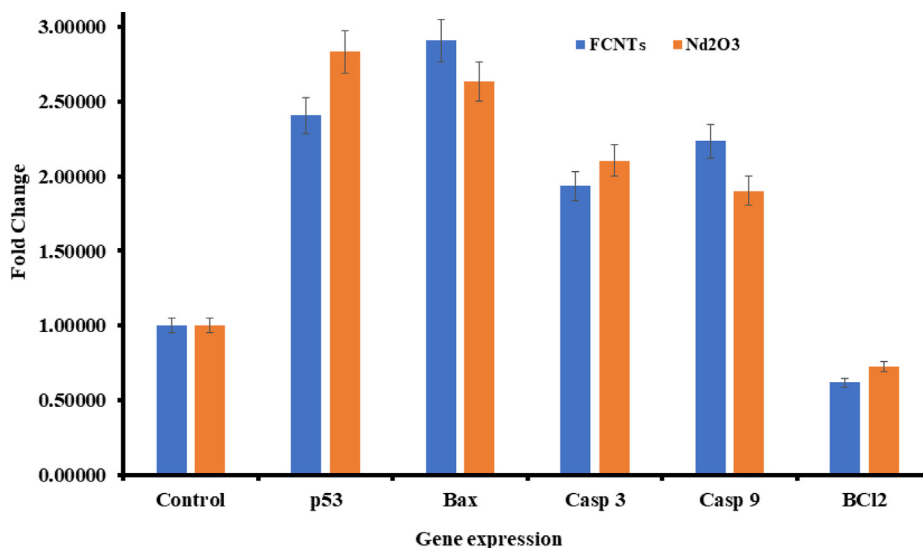


Fig. 8. mRNA expression of apoptosis marker genes by RT-PCR analysis in MCF-7 cells with FCNTs and Nd₂O₃NRs at 50 µg/mL concentration for 24 h with GAPDH gene (used as control). RT-PCR data was achieved with Roche Light Cycler®480 soft-ware (version 1.5). The data is accessible as mean ± SD of three identical experiments with three replicates manner (p < 0.05 for each).

3.8. Reactive Oxygen species (ROS)

A similar and sequential trend were also found in ROS generations noticed in MCF-7 cells after the exposure of FCNTs at 25, 50 and 100 $\mu\text{g}/\text{mL}$ conc for 24 h (Fig. 7). The ROS is increases with the FCNTs and it's evident from the images (Fig. 7A) with control cells. An increase of 118%, 136% and 162% were observed in ROS generation at 25, 50 and 100 $\mu\text{g}/\text{mL}$, as compared to control (Fig. 7B). The ROS is increased with the interaction of $\text{Nd}_2\text{O}_3\text{NRs}$ and it's evident from the images (Fig. 7A) as equated to control cells. The bar chart also evident for ROS with $\text{Nd}_2\text{O}_3\text{NRs}$ in MCF-7 cells after the exposure of NRs at 25, 50 and 100 $\mu\text{g}/\text{mL}$ conc for 24 h (Fig. 7B). An increase of 122, 153 and 189 % were observed in ROS generation at 25, 50 and 100 $\mu\text{g}/\text{mL}$, as compared to control (Fig. 7B) (Garriga et al., 2020).

3.9. Gene expressions study

The real time PCR was also utilized for to understand the mRNA levels of apoptotic and anti-apoptotic marker genes (e.g. p53, bax, caspase-3, caspase-9 and BCL_2) in MCF-7 cells treated with FCNTs and $\text{Nd}_2\text{O}_3\text{NRs}$ at 50 $\mu\text{g}/\text{mL}$ for 24 h. The remarkable changes were examined in mRNA levels in apoptotic markers (p53, Bax, caspase-3, caspase-9 and BCL_2) genes in MCF-7 cells, once exposed (Fig. 8). The mRNA tumor suppression gene favors the apoptosis induction by FCNTs and NRs, scrutinized by the enzymatic activities of caspase-3 at the conc of 50 $\mu\text{g}/\text{ml}$ correspondingly. The obtained results of mRNA gene expression with all chosen genes were in up-regulation except BCL_2 and the fold changes for the p53 (2.4), Bax (2.9), Casp3 (1.9), Casp9 (2.2) and BCL_2 (0.6) in FCNTs whereas in case of $\text{Nd}_2\text{O}_3\text{NRs}$, p53 (2.8), Bax (2.6), Casp3 (2.1), Casp9 (1.9) and BCL_2 (0.7) respectively (Fig. 8). The results represent that NRs induced more as compared to the FCNTs in apoptotic enzymes (caspase-3) (Fig. 8).

4. Conclusions

The conclusion of the present work displayed that a comparative cytological study of carbon nanotubes and neodymium oxide, functionalized and synthesized via solution process and were characterized. The functional CNTs and neodymium oxide nanorods were utilized for cytotoxicity study from low to high concentrations range (1 to 100 $\mu\text{g}/\text{mL}$) against breast cancer cells, which indicates that functional CNTs exhibit less cytological characteristics as compared to neodymium oxide validated by MTT and NRU assays. The work infers that the neodymium oxide exhibit better possibilities to use against cancer cells and these structures will be much effective as compared to available organic/ inorganic based drugs. A detailed investigation is required to testify that the neodymium oxide along with their sustainability under their biological conditions. The study typify that neodymium oxide induces the cytotoxicity, apoptosis in MCF-7 cancer cells via p53, Bax, and caspase pathways, whereas BCL_2 act as anti-apoptotic for cancer cells. It's expected that ROS is increased in cancer cells due to interaction of nanostructures. From the entire experiment and their results it suggest that the neodymium oxide nano structures are much efficient as compared to the functional CNTs and are responsible to control the growth of cancer cells. The nanostructures have the property with their size, which influences to enter in to the cells organelles and reacted fast against cancer cells as likened to the complex structures of drugs. The oxide based nanostructures are cheap and effective and their property makes it more useful against cancer studies and possible to lessen the cost of the preparation of drugs and eases the anxiety of surgery for deprived patient.

Declaration of Competing Interest

The authors declare that they have no known competing financial interests or personal relationships that could have appeared to influence the work reported in this paper.

Acknowledgement

The authors extend their appreciation to the Deputyship for Research & Innovation, Ministry of Education in Saudi Arabia for funding this research (IFKSURC-1-3208).

References

- Ahmad, J., Wahab, R., Siddiqui, M.A., Farshori, N.N., Saquib, Q., Ahmad, N., Al-Khedhairi, A.A., 2022. Neodymium oxide nanostructures and their cytotoxic evaluation in human cancer cells. *J. Trace Elem. Med Biol.* 73, 127029.
- Alghamdi, A., Balkhi, B., Alqahtani, S., Almotairi, H., 2021. The economic burden associated with the management of different stages of breast cancer: a retrospective cost of illness analysis in Saudi Arabia. *Healthcare (Basel)* 9 (7), 907.
- Al-Khedhairi, A.A., Wahab, R., 2022. Silver Nanoparticles: an instantaneous solution for anticancer activity against human liver (HepG2) and breast (MCF-7) cancer cells. *Metals* 12, 148.
- Alshareeda, A.T., Khatijah, M.Z.N., Al-Sowayan, B.S., 2023. Nanotechnology: a revolutionary approach to prevent breast cancer recurrence. *Asian J. Surg.* 46 (1), 13–17.
- Bergsten-Torralba, L.R., Magalhães, D.P., Giese, E.C., Nascimento, C.R.S., Pinho, J.V.A., Buss, D.F., 2022. Toxicity of three rare earth elements, and their combinations to algae, micro crustaceans, and fungi. *Ecotoxicol. Environ. Saf.* 201, 110795.
- Borenfreund, E., Puerner, J.A., 1985. Toxicity determined in vitro by morphological alterations and neutral red absorption. *Toxicology Lett* 24 (2–3), 119–124.
- Breast Cancer Facts & Figures 2019–2020.
- Brouziotis, A.A., Giarra, A., Libralato, G., Pagano, G., Guida, M., Trifuoggi, M., 2022. Toxicity of rare earth elements: an overview on human health impact. *Front. Environ. Sci.* 10, (2022) 948041.
- Czarnecka, J., Wisniewski, M., Forbot, N., Bolibok, P., Terzyk, A.P., Roszek, K., 2020. Cytotoxic or not? Disclosing the toxic nature of carbonaceous nanomaterials through nano-bio interactions. *Materials* 13, 2060.
- Ferlay, J., Parkin, D.M., Steliarova-Foucher, E., 2008. Estimates of cancer incidence and mortality in Europe in 2008. *Eur J Cancer.* 46 (4), 765–781.
- Fujita, K., Obara, S., Maru, J., Endoh, S., 2020. Cytotoxicity profiles of multi-walled carbon nano tubes with different physico-chemical properties. *Toxicol. Mech. Methods* 30 (7), 477–489.
- Garriga, R., Herrero-Contente, T., Palos, M., Cebolla, V.L., Osada, J., Muñoz, E., Rodríguez-Yoldi, M.J., 2020. Toxicity of carbon nanomaterials and their potential application as drug delivery systems: in vitro studies in Caco-2 and MCF-7 cell lines. *Nano Mater.* 10 (8), 1617.
- Humes, S.T., Hentschel, S., Lavelle, C.M., Smith, L.C., Lednický, J.A., Saleh, N.B., Sabo-Attwood, T., 2017. Overcoming qRT-PCR interference by select carbon nanotubes in assessments of gene expression. *Bio techniques* 63 (2), 81–84.
- Kumarathasan, P., Breznan, D., Das, D., Salam, M.A., Siddiqui, Y., Roy, C.M.K., Guan, J., Silva, N.D., Simard, B., Vincent, R., 2015. Cytotoxicity of carbon nanotube variants: a comparative in vitro exposure study with A549 epithelial and J774 macrophage cells. *Nanotoxicology* 9 (2), 148–161.
- Kurvet, I., Juganson, K., Vija, H., Sihtmäe, M., Blinova, I., Syvertsen-Wiig, G., Kahru, A., 2017. Toxicity of nine (doped) rare earth metal oxides and respective individual metals to aquatic microorganisms *Vibrio fischeri* and *tetrahymena thermophile*. *Materials* 10 (7), 754.
- Majhi, K.C., Yadav, M., 2022. Neodymium oxide doped neodymium phosphate as efficient electrocatalyst towards hydrogen evolution reaction in acidic medium. *J. Environ. Chem. Eng.* 10 (3).
- Mosmann, T., 1983. Rapid colorimetric assay for cellular growth and survival: Application to proliferation and cytotoxicity assays. *J. Immunological Methods* 65 (1–2), 55–63.
- München, D.D., Veit, H.M., 2017. Neodymium as the main feature of permanent magnets from hard disk drives (HDDs). *Waste Manag.* 61, 372–376.
- Prajapati, S.K., Malaiya, A., Kesharwani, P., Soni, D., Jain, A., 2022. Biomedical applications and toxicities of carbon nanotubes. *Drug Chem. Toxicol.* 45 (1), 435–450.
- Ramos, S.J., Dinali, G.S., Oliveira, C., Martins, G.C., Moreira, C.G., Siqueira, J.O., Guilherme, L.R.G., 2016. Rare earth elements in the soil environment. *Curr. Pollut. Rep.* 2, 28–50.
- Siddiqui, M.A., Singh, G., Kashyap, M.P., Khanna, V.K., Yadav, S., Chandra, D., Pant, A. B., 2008. Influence of cytotoxic doses of 4-hydroxynonenal on selected neurotransmitter receptors in PC-12 cells. *Toxicol. In Vitro* 22 (7), 1681–1688.
- Siddiqui, M.A., Kashyap, M.P., Kumar, V., Al-Khedhairi, A.A., Musarrat, J., Pant, A.B., 2010. Protective potential of trans-resveratrol against 4-hydroxynonenal induced damage in PC12 cells. *Toxicol. Vitro* 24 (6), 1592–1598.

- Siddiqui, M.A., Ahmad, J., Farshori, N.N., et al., 2013. Rotenone-induced oxidative stress and apoptosis in human liver HepG2 cells. *Mol. Cell. Biochem.* 384 (1–2), 59–69.
- Tang, S., Zheng, C., Chen, M., Du, W., Xu, X., 2020. Geobiochemistry characteristics of rare earth elements in soil and ground water: a case study in Baotou, China. *Sci. Rep.* 10, 11740.
- Vantangoli, M.M., Madnick, S.J., Huse, S.M., Weston, P., Boekelheide, K., 2015. MCF-7 human breast cancer cells form differentiated microtissues in scaffold-free hydrogels. *PLoS One* 10 (8), e0135426.
- Venkataraman, A., Amadi, E.V., Chen, Y., Papadopoulos, C., 2019. Carbon nanotube assembly and integration for applications. *Nanoscale Res. Lett.* 14, 220.
- Wahab, R., Ansari, S.G., Kim, Y.S., Mohanty, T.R., Hwang, I.H., Shin, H.S., 2009. Immobilization of DNA on nano-hydroxyapatite and their interaction with carbon nanotubes. *Synth. Met.* 159 (3–4), 238–245.
- Wahab, R., Siddiqui, M.A., Ahmad, J., Saquib, Q., Al-Khedhairi, A.A., 2021. Cytotoxic and molecular assessment against breast (MCF-7) cancer cells with cobalt oxide nanoballs. *J. King Saud Univ. – Sci.* 33, (5) 101467.
- Wahab, R., Khan, F., Kaushik, N., Kaushik, N.K., Nguyen, L.N., Choi, E.H., Siddiqui, M. A., Farshori, N.N., Saquib, Q., Ahmad, J., Al-Khedhairi, A.A., 2022. L-cysteine embedded core-shell ZnO microspheres composed of nanoclusters enhances anticancer activity against liver and breast cancer cells. *Toxicol. In Vitro* 85, 105460.
- WHO fact-sheet detail for breast cancer 2021. <https://www.who.int/news-room/fact-sheets/detail/breast-cancer>